Formation of Highly Ordered Structure in Poly[(*R*)-3-hydroxybutyrate-*co*-(*R*)-3-hydroxyvalerate] High-Strength Fibers

Toshihisa Tanaka,[†] Masahiro Fujita,[†] Akihisa Takeuchi,[§] Yoshio Suzuki,[§] Kentaro Uesugi,[§] Kazuki Ito,[‡] Tetsuro Fujisawa,[‡] Yoshiharu Doi,[†] and Tadahisa Iwata*[,†]

Polymer Chemistry Laboratory, RIKEN Institute, 2-1 Hirosawa, Wako-shi, Saitama 351-0198, Japan; Japan Synchrotron Radiation Research Institute (JASRI), 1-1-1 Kouto, Sayo-cho, Sayo-gun, Hyogo 679-5198, Japan; and Structural Biochemistry Laboratory, RIKEN Harima Institute, 1-1-1 Kouto, Sayo-cho, Sayo-gun, Hyogo 679-5198, Japan

Received December 26, 2005; Revised Manuscript Received February 20, 2006

ABSTRACT: Biodegradable fibers of poly[(*R*)-3-hydroxybutyrate-*co*-8%-(*R*)-3-hydroxyvalerate] (P(3HB-*co*-8%-3HV)) produced from wild-type bacteria were prepared by melt-spinning, followed in an amorphous state by quenching near the glass transition temperature (T_g). High tensile strength fibers of over 1 GPa were prepared by one-step drawing with small crystal nuclei grown by isothermal crystallization near the T_g. This new drawing technique is a very attractive method for obtaining strong fibers from low-molecular-weight polyesters produced by wild-type bacteria. The highly ordered structure of strong P(3HB-*co*-8%-3HV) fibers was investigated by tensile measurement, scanning electron microscopy, and wide- and small-angle X-ray scatterings (WAXD and SAXS) with synchrotron radiation (SPring-8, Japan). The WAXD patterns of strong fibers showed sharp reflections corresponding to highly oriented α-form (2_1 helix conformation) and β-form (planar zigzag conformation). The weak reflections along the meridian in the SAXS patterns of strong fibers indicate that the density between α- and β-form crystals is nearly identical and that the fibers have highly oriented structure with various thicknesses of α-form lamellar crystals. Furthermore, the microbeam wide-angle X-ray diffraction with Fresnel zone plate optics in synchrotron radiation was performed to investigate the inner structure of the monofilament. It was revealed that strong P(3HB-*co*-8%-3HV) fibers have a uniform structure consistent with two types of molecular conformations: the α-form and β-form crystals. From the results of WAXD and SAXS patterns of one-step-drawn fibers after isothermal crystallization, a new mechanism for the development of β-form crystals is proposed as follows: Many small crystal nuclei in the amorphous region grow slowly during isothermal crystallization near the T_g. The β-form is produced during drawing by the stretching of molecular chains in the constrained amorphous region between small crystal nuclei which act as cross-linking points, and then the α-form lamellar crystals are generated from small crystal nuclei by the crystallization during annealing.

Introduction

Poly[(*R*)-3-hydroxybutyrate] (P(3HB)) and its copolymers are a family of chiral aliphatic polyesters synthesized by a wide variety of bacteria from renewable carbon sources such as sugar and vegetable oil.[1−4] They are the biodegradable plastics that can be mineralized into water and carbon dioxide by bacteria in the environment of soil, seawater, and river water. These microbial polyesters have attracted much attention for use as textile products such as fishing lines or surgical sutures and as a biocompatible thermoplastic with a melting temperature of about 180 °C.[4,5] However, since its moldings deteriorate markedly due to a secondary crystallization with time at room temperature, the materials become stiff and brittle, and it is difficult to produce high tensile strength fiber from bacterial-P(3HB) (weight-average-molecular-weight (M_w) limited to ca. 0.6×10^6).

Some research groups have attempted to improve the mechanical properties of bacterial-P(3HB) fibers. Gordeyev et al. were successful in obtaining P(3HB) fibers with a tensile strength of 190 MPa by annealing after melt spinning.[6] Schmack et al. reported that the tensile strength of high-speed-spun P(3HB) fibers increased to 330 MPa by adding an annealing procedure.[7] Yamane et al. obtained P(3HB) fibers with a tensile strength of 310 MPa by two-step annealing of melt-spun fibers at 110 and 125 °C under constant length.[8] Furuhashi et al. obtained bacterial-P(3HB) fibers with tensile strength of 420 MPa by a combination cold-drawing and two-step-drawing methods; the P(3HB) was drawn at the glass transition temperature in amorphous state and further drawn at higher temperature.[9] However, it has been impossible to develop strong bacterial-P(3HB) fibers with tensile strength for industrial applications (>500 MPa).

Recently, Iwata et al. have succeeded in producing ultrahigh-molecular-weight P(3HB) (UHMW-P(3HB)) ($M_w = (3.3-14) \times 10^6$) under specific fermentation conditions by using a recombinant *Escherichia coli* XL-1 Blue (pSYL105) bacterium.[10] They produced high-strength fibers with a tensile strength of 1.3 GPa from UHMW-P(3HB) by a combination of cold-drawing and two-step-drawing methods.[11] The structure of the high-strength UHMW-P(3HB) monofilament was analyzed by synchrotron radiation microbeam diffraction techniques with a 0.5 μm beam diameter, and it was revealed that the strong UHMW-P(3HB) fiber has a core-sheath structure with two different molecular conformations of P(3HB) chains: 2_1 helix (α-form) and planar zigzag (β-form) conformations.[11] The proper molecular weight for obtaining high tensile strength fibers

[†] RIKEN Institute.
[§] JASRI.
[‡] RIKEN Harima Institute.
* To whom correspondence should be addressed: Tel +81-48-467-9586; Fax +81-48-462-4667; e-mail tiwata@riken.jp.

10.1021/ma0527505 CCC: $33.50
Published on Web 03/17/2006

Scheme 1. Preparation Methods for One-Step-Drawn P(3HB-*co*-8%-3HV) Fibers from Melt-Spinning: (a) One-Step Drawing without Isothermal Crystallization and (b) One-Step Drawing after Isothermal Crystallization

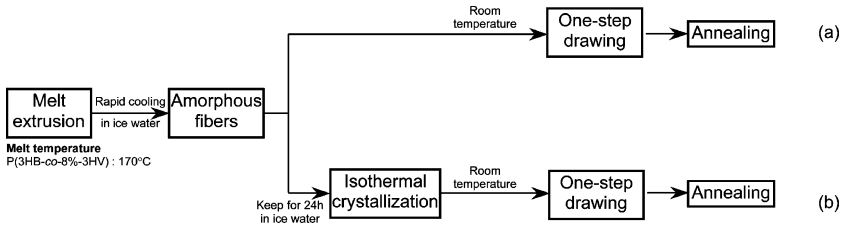

has been limited to ultrahigh-molecular-weight P(3HB) with more than 3.0×10^6 of M_w.

Another method to improve the mechanical properties of P(3HB) fibers and films is to copolymerize P(3HB) with other monomer components.[1,2] Changes of the secondary monomer and component ratio for P(3HB) copolymers show different physical properties. Poly[(*R*)-3-hydroxybutyrate-*co*-(*R*)-3-hydroxyvalerate] (P(3HB-*co*-3HV)) from industrial-scale batch cultures of *Ralstonia eutropha* was provided by Imperial Chemical Industries, U.K., and is well-known among P(3HB) copolymers as the commercial product, Biopol. It has been shown previously that an increase in the proportion of HV to HB monomers decreases the crystallinity and increases the flexibility of the copolymers.[12] Until now, the P(3HB-*co*-3HV) fibers were made by adding some nucleating agents. The presence of a small amount of boron nitride enhances the crystallization rates.[12] Nucleating agents are useful in melt processes such as melt spinning, injection molding, and film blowing where rapid crystallization of the polymer is essential. In addition, the use of boron nitride improves the mechanical properties of P(3HB-*co*-3HV) as a result of reduction in spherulite sizes.[12] The tensile strength of commercial Biopol fiber containing a nucleating agent was reported as 183 MPa.[13] Yamamoto et al. obtained P(3HB-*co*-8%-3HV) fibers with tensile strengths of 210 MPa containing nucleating agents by simultaneous drawing and annealing after spinning.[14] However, there has been no report on the production of strong fibers of bacterial-P(3HB-*co*-8%-3HV) without nucleating agents or on the effect of drawing conditions on the development of highly ordered structure in this polymer.

In the present paper, we report the production of high tensile strength fibers of bacterial-P(3HB-*co*-8%-3HV) of low molecular weight without nucleating agents. Strong bacterial-P(3HB-*co*-8%-3HV) fibers were obtained by one-step-drawing with small crystal nuclei grown by slow crystallization during isothermal crystallization near the glass transition temperature. The highly ordered structure of the P(3HB-*co*-8%-3HV) monofilament was analyzed by wide- and small-angle X-ray scatterings and by synchrotron radiation microbeam diffraction with Fresnel zone plate optics at the SPring-8 synchrotron radiation facility in Japan. A new generation mechanism of highly ordered structure will be proposed on the basis of the X-ray diffraction study.

Experimental Section

Materials. Bacterial-poly[(*R*)-3-hydroxybutyrate-*co*-8%-(*R*)-3-hydroxyvalerate] (P(3HB-*co*-8%-3HV)) with a M_w and polydispersity of 1.0×10^6 and 2.8, respectively, was supplied by Monsanto Japan Co. After dissolution in chloroform at 100 °C the samples were purified by precipitation in *n*-hexane and dried under vacuum. The melting temperature (T_m) and glass transition temperature (T_g) of the P(3HB-*co*-8%-3HV) powder were found to be 143 and −4 °C, respectively, as measured by differential scanning calorimetry. The mol % composition (7.7%) of the 3HV repeating unit was determined by ^{1}H nuclear magnetic resonance (^{1}H NMR) in $CDCl_3$.

Preparation of Fibers. Melt-spinning of bacterial-P(3HB-*co*-8%-3HV) was carried out using a laboratory-size extruder (IMC-1149, Imoto Machinery Co. Ltd., Japan) equipped with a single nozzle with an inner diameter of 1 mm. Bacterial-P(3HB-*co*-8%-3HV) was extruded at 170 °C, which was 30 °C higher than the T_m. The molten extruded polymer was taken up at 50−60 mm/s by roll and directly quenched into ice water bath placed 15 cm below the nozzle to obtain the amorphous fibers. The extrusion rate was 0.1−0.2 mm/s. Drawing procedures from the amorphous fiber were conducted as shown in Scheme 1.

Drawing methods used are (a) one-step-drawing by using a stretching machine at room temperature without isothermal crystallization and (b) one-step-drawing by using a stretching machine at room temperature after isothermal crystallization for a constant period in an ice water bath of near the T_g. The drawing rate by stretching machine was 4.5−5.0 mm/s. To increase the crystallinity, all fibers were annealed at 60 °C in a hot oven under constant tension for 30 min. All samples were analyzed after aging at room temperature for at least 1 week. The diameter of fibers was 30−240 μm.

Analytical Procedures. Mechanical properties of fibers were evaluated by using a tensile testing machine (Shimadzu EZTest). Initial specimen lengths were 10 mm, and tests were carried out at a cross-head speed of 20 mm/min at room temperature. These results were averaged for five samples for each condition.

Scanning electron micrographs for the surface on samples were taken by using a JEOL JSM-6330F microscope, operated at an acceleration voltage of 5 kV, after samples were coated with gold using a SANYU DENSHI SC-701 quick coater.

The two-dimension wide-angle diffraction (WAXD) and small-angle X-ray scattering (SAXS) experiments were carried out using beamline BL45XU with a wavelength of 0.09 nm at the SPring-8 synchrotron radiation facility in Japan. A P(3HB-*co*-8%-3HV) monofilament was set perpendicular to the X-ray beam and parallel to the detector. The diffraction patterns were recorded with a charge-coupled-device (CCD) camera (C7300-10-12NR, Hamamatsu Photonics, Japan) with exposure times of 76−1058 ms. The pixel size for the CCD camera was 125 μm × 125 μm. The number of bits per pixel was 12 bits. The camera lengths for WAXD and SAXS were 150 and 2200 mm, respectively.

The microbeam wide-angle X-ray diffraction was carried out using beamline BL47XU with a wavelength of 0.15497 nm in 8 keV at the SPring-8 synchrotron radiation facility in Japan. A focal spot size of 0.5 μm was generated by Fresnel zone plate optics.[15] The P(3HB-*co*-8%-3HV) fiber was linearly scanned perpendicular to the fiber axis with a step width of 4 μm between the individual frames. The diffraction patterns were recorded with a CCD camera (C4880-10-14A, Hamamatsu Photonics, Japan) with an exposure time of 10 s. The pixel size for the CCD camera was 150 μm × 150 μm. The number of bits per pixel was 14 bits. The camera length was 110 mm.

WAXD measurements were made to estimate the degree of orientation of the crystallites and the degree of crystallinity. The degree of orientation of the crystallites (f_c) is evaluated in terms of the following equation by using azimuthal breadth analysis:

$$f_c = (180° - \beta_c)/180°$$

The β_c was determined from the half-width of the azimuthal

Table 1. Mechanical Properties, Crystal Orientation, Crystallinity, and Long Period of One-Step-Drawn P(3HB-*co*-8%-3HV) Fibers without or after Isothermal Crystallization near the Glass Transition Temperature

draw ratio	isothermal crystallization	tensile strength (MPa)	elongation to break (%)	Young's modulus (GPa)	crystal orientation	crystallinity (%)	long period (nm)
as-spun	−	28	13	1.1	−	62	6
10	−	90	76	2.0	0.90	70	6
nondrawn	+	27	15	1.2	−	64	6
5	+	710	50	6.8	0.94	73	7
10	+	1065	40	8.0	0.95	83	−[a]

[a] Not detected due to weak reflection.

Table 2. Mechanical Properties of Fibers Processed from P(3HB) Homopolymer and Copolymers

sample	tensile strength (MPa)	elongation to break (%)	Young's modulus (GPa)	ref
bacterial-P(3HB-*co*-3HV) ($M_w = 1.0 \times 10^6$)	183	6.5	9.0	13
	210	30	1.8	14
	1065	40	8.0	this study
bacterial-P(3HB) ($M_w = 0.6 \times 10^6$)	190	54	5.6	6
	330	37	7.7	7
	310	60	3.8	8
	416	24	5.2	9
UHMW-P(3HB) ($M_w = 5.3 \times 10^6$)	1320	35	18.1	11
bacterial-P(3HB-*co*-4HB) ($M_w = 0.3 \times 10^6$)	545	60	0.7	17
bacterial-P(3HB-*co*-3HH) ($M_w = 1.9 \times 10^6$)	46	200	−	18

direction of equatorial (020) reflection in the WAXD patterns of drawn fibers. The degree of crystallinity can be estimated using a two-phase model of the polymer structure in which the measured intensity is a linear combination of the intensities from the crystalline and the amorphous regions.[16] All data in the two-dimension WAXD pattern were integrated along the azimuthal direction from 0° to 360° for all diffraction angles (2θ) to convert into one dimension profile by circular averaging. The crystallinity was calculated from the ratio of integrals for the crystalline and amorphous areas to the overall intensity of the first dimensional profile according to Vonk's method.[16]

SAXS measurement can estimate the long period attributed to the spacing of lamellar stacks. The long periods were determined by using Bragg's equation ($L = \lambda/(2 \sin \theta)$) from the maximum peak along the meridional scattering of the SAXS patterns.

Results and Discussion

Mechanical Properties and Morphology. Isothermal crystallization of amorphous P(3HB-*co*-8%-3HV) fiber was held in ice water for a certain period to prevent rapid crystallization and grow small crystal nuclei. One-step drawing after isothermal crystallization was performed with a stretching machine at room temperature, followed by an annealing step at 60 °C for 30 min in a hot oven in order to fix the extended polymer chains (Scheme 1b). One-step-drawn fibers that were isothermally crystallized for 24 h were opaque, and their maximum total draw ratio was ca. 10 times with initial length of sample. To compare the effects of isothermal crystallization, one-step drawing without isothermal crystallization was performed by the stretching machine at room temperature (Scheme 1a).

The mechanical properties of one-step-drawn fibers of P(3HB-*co*-8%-3HV) without or after isothermal crystallization are summarized in Table 1. The tensile strength of as-spun fibers was ca. 30 MPa independent of isothermal crystallization. The tensile strength of a 10 times one-step-drawn fiber without isothermal crystallization was 90 MPa. However, the tensile strength of a 5 times one-step-drawn fiber after isothermal crystallization increased to 710 MPa. Moreover, the tensile strength of a 10 times one-step-drawn fiber after isothermal crystallization further increased to 1065 MPa. The mechanical properties of one-step-drawn fibers after isothermal crystallization are much higher than those reported previously for this polymer.[13,14] Mechanical properties of fibers processed from P(3HB) homopolymer and other copolymers such as poly[(*R*)-3-hydroxybutyrate-*co*-4-hydroxybutyrate] (P(3HB-*co*-4HB))[17] and poly[(*R*)-3-hydroxybutyrate-*co*-(*R*)-3-hydroxyhexanoate] (P(3HB-*co*-3HH))[18] reported previously are listed in Table 2. This new drawing method after isothermal crystallization near glass transition temperature is an attractive procedure to obtain strong fibers from low-molecular-weight polyesters produced by wild-type bacteria.

Figure 1 shows the scanning electron micrographs of P(3HB-*co*-8%-3HV) fibers prepared by one-step-drawing without isothermal crystallization. The surface of the as-spun fiber without isothermal crystallization was smooth throughout the fiber (Figure 1a,a′). However, the surface of the 10 times one-step-drawn fiber without isothermal crystallization by stretching at room temperature was irregular and had fibril-like lines parallel to the drawing direction (Figure 1b,b′).

The scanning electron micrographs of P(3HB-*co*-8%-3HV) fibers prepared by one-step-drawing after isothermal crystallization are shown in Figure 2. The surface of nondrawn fiber after isothermal crystallization was smooth throughout the fiber (Figure 2a,a′) as was the case of the as-spun fiber without isothermal crystallization. The surfaces of 5 and 10 times one-step-drawn fibers after isothermal crystallization had many fine voids that were evenly distributed throughout the fiber (Figure 2b,c,b′,c′), unlike the fibril-like lines generated in the direction of the 10 times one-step-drawn fibers (Figure 1b,b′).

Structure Analysis by Wide- and Small-Angle X-ray Diffraction. To analyze the highly ordered structure of one-step-drawn P(3HB-*co*-8%-3HV) fibers, wide- and small-angle X-ray scatterings (WAXD and SAXS) were performed with synchrotron radiation at SPring-8. Figure 3 shows the WAXD and SAXS patterns of one-step-drawn P(3HB-*co*-8%-3HV) fibers without isothermal crystallization. The WAXD and SAXS patterns of the as-spun fiber without isothermal crystallization showed ring and four-point patterns, respectively, indicating that the α-form crystals with 2_1 helix conformation[19,20] of P(3HB) are unoriented and inclined (Figure 3a,a′).

The WAXD pattern of a 10 times one-step-drawn fiber without isothermal crystallization showed the arc reflections of the α-form (Figure 3b), indicating the low orientation of α-form crystals along the drawing direction. The (020) orientation of 10 times one-step-drawn fiber without isothermal crystallization was 0.90. The crystallinities of as-spun and 10 times one-step-drawn fibers without isothermal crystallization were 62% and 70%, respectively (Table 1). The SAXS pattern of 10 times one-

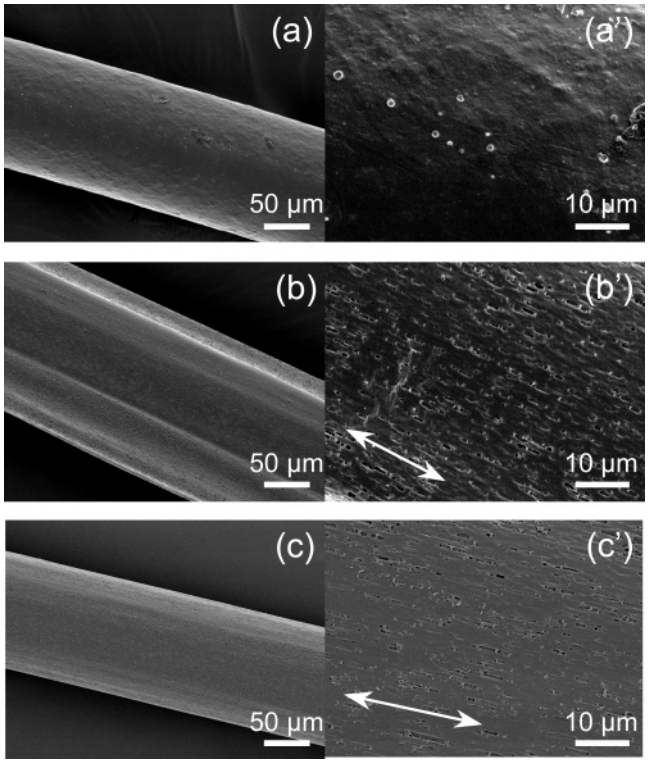

Figure 2. Scanning electron micrographs of P(3HB-*co*-8%-3HV) fibers after isothermal crystallization: (a, a′) nondrawn, (b, b′) 5 times one-step-drawn at room temperature, and (c, c′) 10 times one-step-drawn at room temperature. The arrows indicate the drawing direction.

step-drawn fiber without isothermal crystallization showed clear two-spot reflections along the meridian corresponding to oriented lamellae parallel to the drawing direction (Figure 3b′), indicating the constant periodicity of lamellar crystals. The long period of a typical 10 times one-step-drawn fiber without isothermal crystallization was 6 nm.

Figure 4 shows the WAXD and SAXS patterns of one-step-drawn P(3HB-*co*-8%-3HV) fibers after isothermal crystallization. The WAXD pattern of a nondrawn fiber after isothermal crystallization showed only a ring pattern indicative of the unoriented α-form crystal (Figure 4a) as observed with the as-spun fiber without isothermal crystallization. However, the WAXD patterns of 5 and 10 times one-step-drawn fibers after

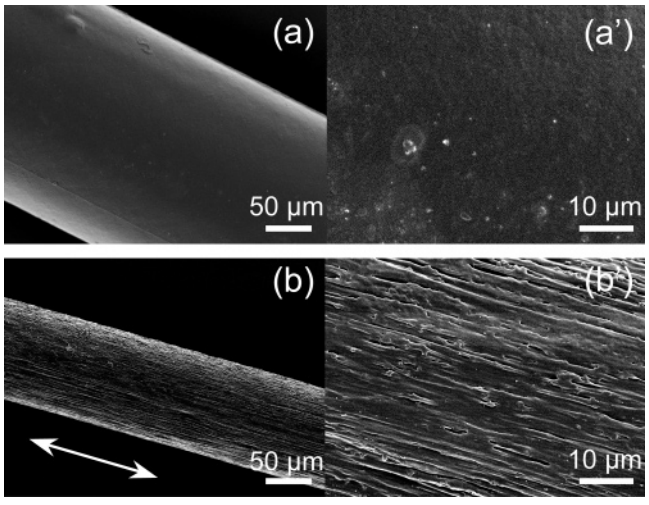

Figure 1. Scanning electron micrographs of P(3HB-*co*-8%-3HV) fibers without isothermal crystallization: (a, a′) as-spun and (b, b′) 10 times one-step-drawn at room temperature. The arrow indicates the drawing direction.

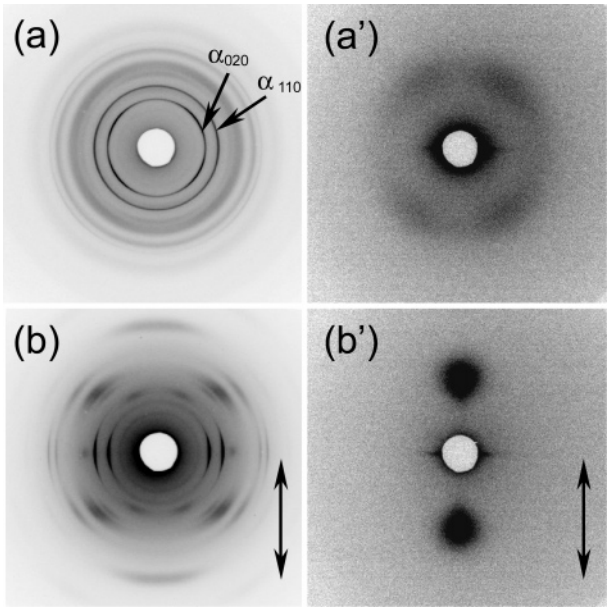

Figure 3. WAXD and SAXS patterns of P(3HB-*co*-8%-3HV) fibers without isothermal crystallization: (a, a′) as-spun and (b, b′) 10 times one-step-drawn at room temperature. Left and right rows represent the WAXD and SAXS patterns. The vertical arrows indicate the direction of fiber axis.

isothermal crystallization showed the sharp reflections of both the α-form and *β*-form with a planar zigzag conformation of P(3HB)[21] along the equator (Figure 4b,c). The orientation of α-form crystals and the intensity of *β*-form reflection increased with increasing draw ratio for one-step-drawn fibers after isothermal crystallization. The (020) orientations of 5 and 10 times one-step-drawn fibers after isothermal crystallization were 0.94 and 0.95, respectively. The intensity of the *β*-form reflection along the equator showed a clear increase in intensity with increasing draw ratio for the correcting profile as the standard intensity of the (020) reflection (Figure 5). The crystallinities of nondrawn and 5 and 10 times one-step-drawn fibers after isothermal crystallization were 64, 73, and 83%, respectively, summarized in Table 1. The orientation and crystallinity of fibers after isothermal crystallization were higher compared to those of fibers without isothermal crystallization. Many small crystal nuclei grow by slow crystallization during the isothermal crystallization near the glass transition temperature. Drawing after isothermal crystallization leads to an increase in the orientation and crystallization of the molecular chains in the constrained amorphous region between these small crystal nuclei.

The SAXS pattern of a nondrawn fiber after isothermal crystallization showed only a ring pattern arising from unoriented lamellae (Figure 4a′) similar to the as-spun fiber without isothermal crystallization. The SAXS patterns of 5 and 10 times one-step-drawn fibers after isothermal crystallization (Figure 4b′,c′) showed clear streak scatterings along the equator and the weak scattering along the meridian. The clear streak scatterings along the equator suggest that many voids exist in one-step-drawn fibers as observed by scanning electron micrographs in Figure 2b′,c′. The intensity of the meridional reflection in the SAXS patterns decreased with increasing draw ratio, as shown in Figure 6. From the intensity of the meridional reflections corresponding to the lamellar crystals oriented toward the drawing direction, the long periods of nondrawn and 5 times one-step-drawn fibers after isothermal crystallization were determined to be 6 and 7 nm, respectively (Table 1). However, because the intensity of the meridional reflection in the SAXS

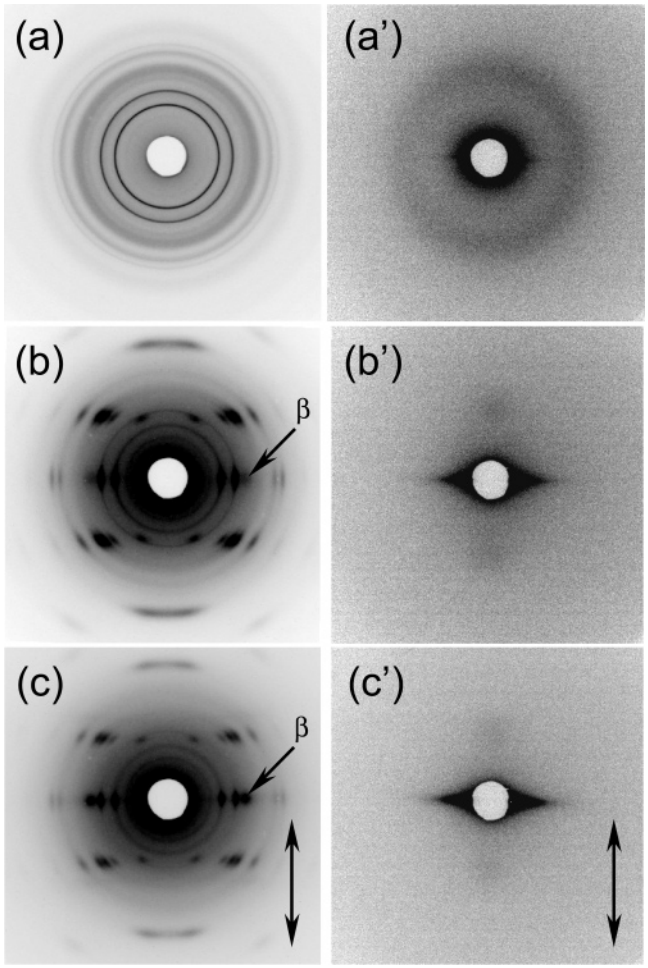

Figure 4. WAXD and SAXS patterns of P(3HB-*co*-8%-3HV) fibers after isothermal crystallization: (a, a′) nondrawn, (b, b′) 5 times one-step-drawn at room temperature, and (c, c′) 10 times one-step-drawn at room temperature. Left and right rows represent the WAXD and SAXS patterns. The arrows indicate a reflection derived from the β-form with planar zigzag conformation. The vertical arrows indicate the direction of fiber axis.

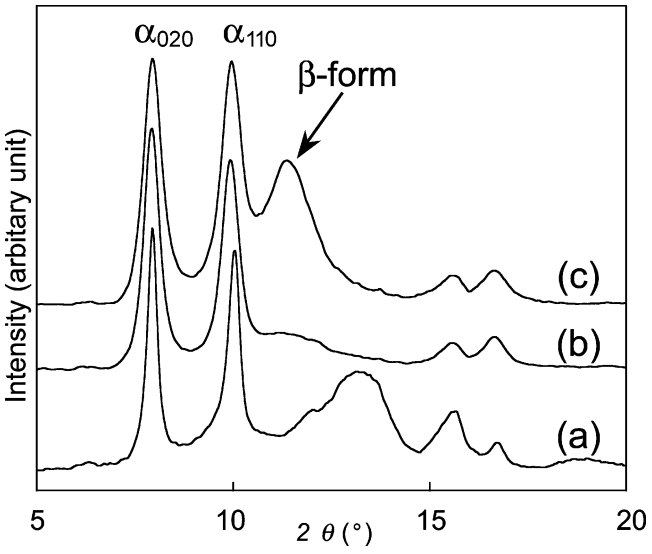

Figure 5. Linear WAXD profiles obtained from the equatorial scans in 2D WAXD patterns of P(3HB-*co*-8%-3HV) fibers after isothermal crystallization: (a) nondrawn, (b) 5 times one-step-drawn at room temperature, and (c) 10 times one-step-drawn at room temperature.

pattern of the 10 times one-step-drawn fibers was very weak, the long period could not be determined. This weak reflection

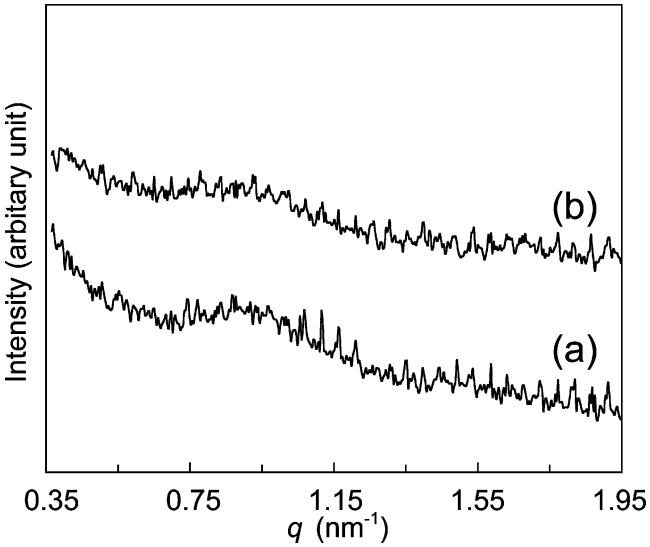

Figure 6. Linear SAXS profiles obtained from the meridional scans in 2D SAXS patterns of P(3HB-*co*-8%-3HV) fibers after isothermal crystallization: (a) 5 times one-step-drawn at room temperature and (b) 10 times one-step-drawn at room temperature. The scattering vector q is defined by $q = (4\pi/\lambda) \sin \theta$.

along the meridian indicates that the density between α- and β-form crystals is nearly identical and that the one-step-drawn fibers after isothermal crystallization have a highly oriented structure with various thicknesses of α-form lamellar crystals. This observation indicates that the β-form crystals with planar zigzag conformation first develop during the drawing process by the stretching of the molecular chains followed by the generation of α-form lamellar crystals during the annealing process by crystallization.

Structure Analysis by Microbeam X-ray Diffraction of Monofilaments. Microbeam X-ray diffraction with beam sizes in the micrometer range is a useful and powerful method to investigate the in situ transition of the crystalline region and the local structure for monofilaments. Microdiffraction techniques have been developed mainly at the ID13 beamline of the European Synchrotron Radiation Facility (ERSF) with a beam size of 3−10 μm to analyze whole fibers during stretching and extrusion such as viscose rayon fibers,[22] spider silk,[23] twisting lamellar crystals, such as spherulites of P(3HB),[24] and a poly(lactic acid)/atactic-P(3HB) blend.[25] Recently, we developed the microdiffraction techniques with a focal spot size of 0.5 μm at the SPring-8 synchrotron radiation facility for analysis of the UHMW-P(3HB) monofilament[11] and P(3HB) copolymer spherulites.[26] Previous results for monofilaments showed that the drawn fibers had a core-sheath structure with differences of the size or orientation distribution of the crystalline region, while results for spherulites indicated that the structural changes were directly correlated with the morphological feature responsible for banding by twisting lamellar crystals. Such morphological differences are best investigated with a beam size which is significantly smaller than the size of the samples. Therefore, to reveal the detailed fiber structure and the distribution of two molecular conformations in drawn P(3HB-*co*-8%-3HV) monofilament, a microbeam X-ray diffraction experiment was performed at the SPring-8 synchrotron radiation facility in Japan. The beam size was focused to 0.5 μm using Fresnel zone plate optics,[15] and the P(3HB-*co*-8%-3HV) monofilament was scanned linearly and perpendicular to the fiber axis with a step of 4 μm.

Figure 7 shows a series of microbeam X-ray diffraction patterns for one-step-drawn P(3HB-*co*-8%-3HV) fiber after isothermal crystallization (120 μm diameter) scanned perpen-

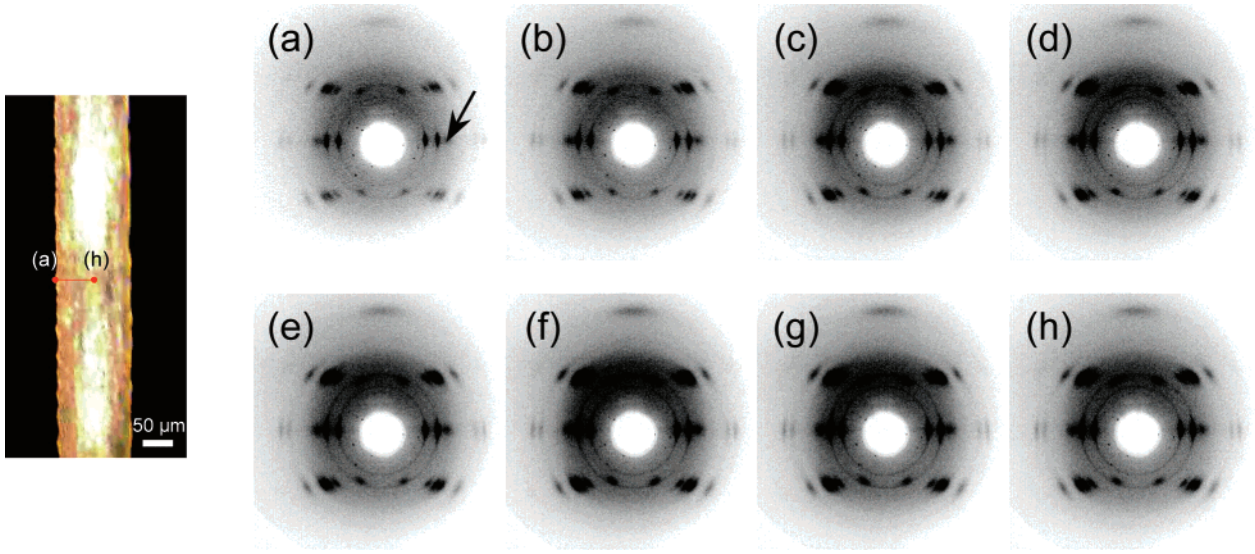

Figure 7. Microbeam X-ray diffraction patterns of 10 times one-step-drawn P(3HB-*co*-8%-3HV) fiber ($\phi = 120$ μm) after isothermal crystallization recorded from the line area in the microscope image (left picture). These patterns were recorded at each distance from the edge of fiber: (a) 0, (b) 8, (c) 16, (d) 24, (e) 32, (f) 40, (g) 48, and (h) 56 μm.

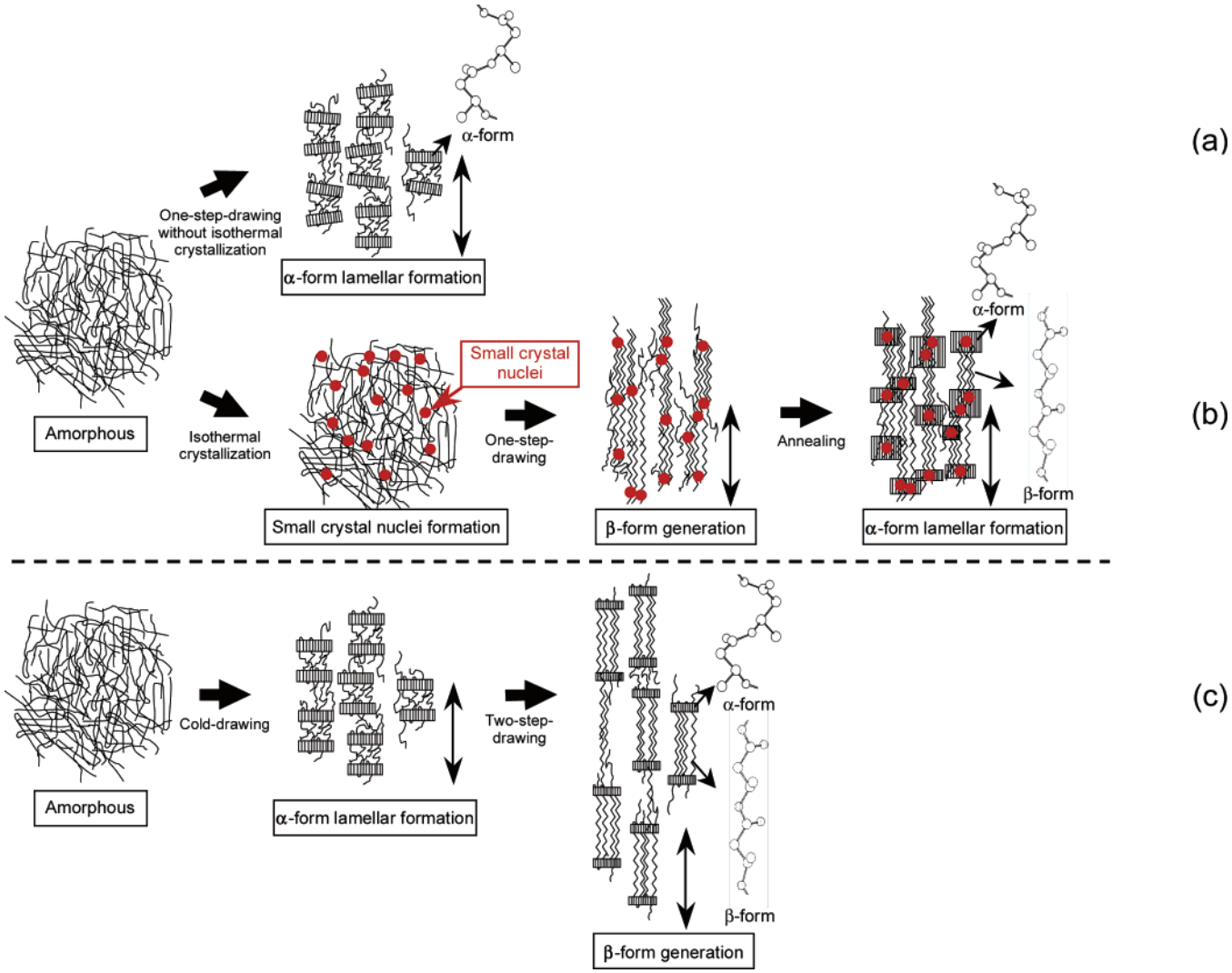

Figure 8. New mechanism for generating the planar zigzag conformation (β-form) in high-strength P(3HB-*co*-3HV) fibers by different drawing methods: (a) one-step-drawing without isothermal crystallization, (b) one-step-drawing after isothermal crystallization, and (c) cold-drawing and two-step-drawing.[11,28−30] The vertical arrows indicate the drawing direction.

dicular to the fiber axis. All microbeam X-ray diffraction patterns of one-step-drawn fiber showed reflections for both the α- and β-form crystals. These reflections were constant throughout the fiber but changed in intensity dependent on the thickness of the sample. The (020) orientation and crystallinity data of the one-step-drawn fibers after isothermal crystallization were

obtained from the intensity of the diffraction patterns and were similar for all samples, indicating that one-step-drawn P(3HB-*co*-8%-3HV) fibers after isothermal crystallization do not have the core-sheath structure observed in cold-drawn and two-step-drawn UHMW-P(3HB) fibers.[11] In other words, one-step-drawn P(3HB-*co*-8%-3HV) fibers after isothermal crystallization have a uniform structure throughout consistent with both highly oriented α- and *β*-form crystals. This structure supports the result that one-step-drawn fibers after isothermal crystallization have high tensile strength despite their low draw ratio.

The (020) and (110) reflections in the microbeam X-ray diffraction patterns of a one-step-drawn fiber are observed in the ring patterns, as shown in Figure 7. These ring patterns are derived from pseudohexagonal crystals oriented perpendicular to the fiber axis, as reported by Furuhashi et al.[27]

New Mechanism for Generating the Planar Zigzag Conformation (*β*-Form). The presence of the *β*-form crystals with a planar zigzag conformation is an important factor to generate high-strength P(3HB) materials. The existence of *β*-form crystals is only observed by wide-angle X-ray diffraction[21] and cannot be provided by other analytical mean, such as DSC measurements. Until now, the only known mechanism for generating the highly ordered *β*-form structure was derived from the observations of the cold-drawn and two-step-drawn UHMW-P(3HB) fibers[11,28] and films.[29,30] This mechanism proposed that the α-form with lamellar crystals is produced by cold-drawing and then the *β*-form with planar zigzag conformation developed during the stretching in the second dimension of the constrained amorphous chains between α-form crystals, as shown in Figure 8c. However, from the results of WAXD and SAXS patterns in one-step-drawn P(3HB-*co*-8%-3HV) fibers after isothermal crystallization, the mechanism for generating α- and *β*-form crystals is likely to be different from the case of cold-drawn and two-step-drawn fibers. A new mechanism for the development of *β*-form crystals for one-step-drawn P(3HB-*co*-8%-3HV) fibers after isothermal crystallization is proposed as follows: (1) many small crystal nuclei grow in the amorphous region by slow crystallization during isothermal crystallization near the T_g, (2) the *β*-form is developed first by the stretching of molecular chains in the constrained amorphous region between small crystal nuclei, which act as cross-linking points, and then (3) the α-form lamellar crystals with various thicknesses are generated from the small crystal nuclei during annealing, as shown in Figure 8b.

Conclusions

High tensile strength fibers of bacterial-P(3HB-*co*-8%-3HV) were prepared from amorphous states by one-step-drawing at room temperature after isothermal crystallization at the T_g by slow crystallization. The 10 times one-step-drawn bacterial-P(3HB-*co*-8%-3HV) fiber after isothermal crystallization has a tensile strength of 1065 MPa and is equal to that of common polymers such as polyethylene or poly(ethylene terephthalate).

The molecular and highly ordered structures of one-step-drawn P(3HB-*co*-8%-3HV) fibers were analyzed by the wide- and small-angle X-ray scatterings and microbeam X-ray diffraction (beam size of 0.5 *μ*m) with Fresnel zone plate optics at the SPring-8 synchrotron radiation facility in Japan. It was revealed that the one-step-drawn P(3HB-*co*-8%-3HV) fiber after isothermal crystallization has a uniform structure, consistent with a highly oriented 2_1 helix conformation (α-form) and planar zigzag conformation (*β*-form). The *β*-form in one-step-drawn P(3HB-*co*-8%-3HV) fibers after isothermal crystallization is produced by the stretching of molecular chains in the amorphous region between small crystal nuclei which act as cross-linking points followed by the generation of the α-form during annealing. This mechanism for generating the α- and *β*-forms is different from previously described cold-drawn and two-step-drawn fibers[11,28] and films.[21,29,30]

This one-step-drawing after isothermal crystallization near the glass transition temperature is a very useful procedure that can be applied to bacterial-P(3HB-*co*-3HV) fibers and other biodegradable aliphatic polyester fibers, as shown in Table 2.

Acknowledgment. This work has been supported by a Grant-in-Aid for Young Scientists (A) from the Ministry of Education, Culture, Sports, Science and Technology (MEXT) of Japan (No. 15685009) (to T. Iwata) and by a grant for Ecomolecular Science Research provided by RIKEN Institute. The authors are grateful to T. Sawayanagi of the Tokyo Institute of Technology and C. T. Nomura of the State University of New York-College of Environmental Science and Forestry for their assistances. The synchrotron radiation experiments were performed at the SPring-8 with the approval of the Japan Synchrotron Radiation Research Institute (JASRI) (Proposal No. 2003B0054-NL2b-np and No. 2004B0016-ND1b-np).

References and Notes

(1) Holmes, P. A. In *Developments in Crystalline Polymers*; Bassett, D. C., Ed.; Elsevier Applied Science: London, 1988; Vol. 2, pp 1−65.
(2) Doi, Y. In *Microbial Polyesters*; VCH Publishers: Weinheim, 1990.
(3) Anderson, A. J.; Dawes, E. A. *Microbiol. Rev.* **1990**, *54*, 450.
(4) Lenz, R. W.; Marchessault, R. H. *Biomacromolecules* **2005**, *6*, 1.
(5) Lemoigne, M. *Ann. Inst. Pasteur.* **1925**, *39*, 144.
(6) Gordeyev, S. A.; Nekrasov, Y. P. *J. Mater. Sci., Lett.* **1999**, *18*, 1691.
(7) Schmack, G.; Jehnichen, D.; Vogel, R.; Tandler, B. *J. Polym. Sci., Part B: Polym. Phys.* **2000**, *38*, 2841.
(8) Yamane, H.; Terao, K.; Hiki, S.; Kimura, Y. *Polymer* **2001**, *42*, 3241.
(9) Furuhashi, Y.; Imamura, Y.; Jikihara, Y.; Yamane, H. *Polymer* **2004**, *45*, 5703.
(10) Kusaka, S.; Iwata, T.; Doi, Y. *J. Macromol. Sci., Pure Appl. Chem.* **1998**, *A35*, 319.
(11) Iwata, T.; Aoyagi, Y.; Fujita, M.; Yamane, H.; Doi, Y.; Suzuki, Y.; Takeuchi, A.; Uesugi, K. *Macromol. Rapid Commun.* **2004**, *25*, 1100.
(12) Marchessault, R. H.; Bluhm, T. L.; Deslandes, Y.; Hamer, G. K.; Orts, W. J.; Sundararajan, J. R.; Taylor, M. G.; Bloembergen, S.; Holden, D. A. *Macromol. Chem. Macromol. Symp.* **1988**, *19*, 235.
(13) Ohura, T.; Aoyagi, Y.; Takagi, K.; Yoshida, Y.; Kasuya, K.; Doi, Y. *Polym. Degrad. Stab.* **1999**, *63*, 23.
(14) Yamamoto, T.; Kimizu, M.; Kikutani, T.; Furuhashi, Y.; Cakmak, M. *Int. Polym. Process.* **1997**, *XII*, 29.
(15) Suzuki, Y.; Takeuchi, A.; Takano, H.; Ohigashi, T.; Takenaka, T. *Jpn. J. Appl. Phys.* **2001**, *40*, 1508.
(16) Vonk, C. G. *J. Appl. Crystallogr.* **1973**, *6*, 148.
(17) Martin, D. P.; Williams, S. F. *Biochem. Eng. J.* **2003**, *16*, 97.
(18) Bond, E. B. *Macromol. Symp.* **2003**, *197*, 19.
(19) Yokouchi, M.; Chatani, Y.; Tadokoro, H.; Teranishi, K.; Tani, K. *Polymer* **1973**, *14*, 267.
(20) Okamura, K.; Marchessault, R. H. In *Conformation of Biopolymers*; Romachandra, G. N., Ed.; Academic Press: New York, 1967; Vol. 2, pp 709−720.
(21) Orts, W. J.; Marchessault, R. H.; Bluhm, T. L.; Hamer, G. K. *Macromolecules* **1990**, *23*, 5368.
(22) Muller, M.; Riekel, C.; Vuong, R.; Chanzy, H. *Polymer* **2000**, *41*, 2627.
(23) Riekel, C.; Madsen, B.; Knight, D.; Vollrath, F. *Biomacromolecules* **2000**, *1*, 622.
(24) Gazzano, M.; Focarete, M. L.; Riekel, C.; Scandola, M. *Biomacromolecules* **2000**, *1*, 604.
(25) Gazzano, M.; Focarete, M. L.; Riekel, C.; Scandola, M. *Biomacromolecules* **2004**, *5*, 553.
(26) Tanaka, T.; Fujita, M.; Takeuchi, A.; Suzuki, Y.; Uesugi, K.; Doi, Y.; Iwata, T. *Polymer* **2005**, *46*, 5673.
(27) Furuhashi, Y.; Ito, H.; Kikutani, T.; Yamamoto, T.; Kimizu, M.; Cakmak, M. *J. Polym. Sci., Part B: Polym. Phys.* **1998**, *36*, 2471.
(28) Iwata, T.; Fujita, M.; Aoyagi, Y.; Doi, Y.; Fujisawa, T. *Biomacromolecules* **2005**, *6*, 1803.
(29) Aoyagi, Y.; Doi, Y.; Iwata, T. *Polym. Degrad. Stab.* **2003**, *79*, 209.
(30) Iwata, T.; Tsunoda, K.; Aoyagi, Y.; Kusaka, S.; Yonezawa, N.; Doi, Y. *Polym. Degrad. Stab.* **2003**, *79*, 217.

MA0527505